

HM3D-ABO: A Photo-realistic Dataset for Object-centric Multi-view 3D Reconstruction

Technical Report

Zhenpei Yang* Zaiwei Zhang Qixing Huang
The University of Texas at Austin

Abstract

Reconstructing 3D objects is an important computer vision task that has wide application in AR/VR. Deep learning algorithm developed for this task usually relies on an unrealistic synthetic dataset, such as ShapeNet [7, 9] and Things3D [42]. On the other hand, existing real-captured object-centric datasets usually do not have enough annotation to enable supervised training or reliable evaluation. In this technical report, we present a photo-realistic object-centric dataset HM3D-ABO. It is constructed by composing realistic indoor scene [29] and realistic object [10]. For each configuration, we provide multi-view RGB observations, a water-tight mesh model for the object, ground truth depth map and object mask. The proposed dataset could also be useful for tasks such as camera pose estimation and novel-view synthesis. The dataset generation code is released at <https://github.com/zhenpeiyang/HM3D-ABO>.

1. Introduction

Reconstructing 3D object has been studied for decades [3, 19, 21, 27, 28, 39, 43–45, 50] and has been receiving more and more interest due to the recent popularity AR/VR applications. With multi-view renderings from object model collection datasets [7, 10, 12, 14, 30, 41], researchers can develop data-driven approaches for object reconstruction but the clean backgrounds introduce a domain gap with real-world images. Things3D [42] has tried to attach different backgrounds to those object renderings by placing CAD models in synthetic 3D indoor scenes. However, their renderings of synthetic indoor environments is still far from realistic. On the other hand, several works have also tried to create 3D object annotations from real 2D images, such as Pix3D [35] and Scan2CAD [2]. Yet these works either only provide a single-view image [35] setting or does not provide an accurate 3D model [2]. Redwood [8] contains multi-view 2D images and 3D depth scans but it only provides reconstructed 3D models for very few instances. Recently, Google Objectron [1] dataset has released a collection of short, object-centric video clips

* yzp@utexas.edu

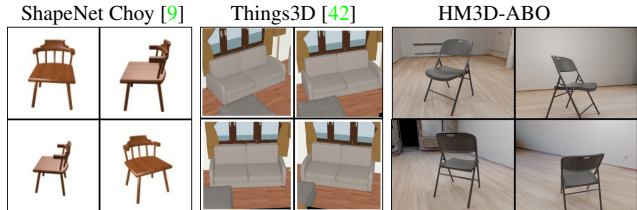


Figure 1. Qualitative comparison among three object-centric multi-view datasets. Our proposed HM3D-ABO dataset has both realistic foreground objects and realistic background scenes.

with 3D object-level annotations but it does not provide reconstructed 3D models. In light of the challenge of creating accurate annotations for real-world object scans, in this technical report, we propose an approach to generate a photo-realistic object-centric dataset based on existing high-quality scene and object models.

2. HM3D-ABO Dataset

Dataset Assets. In order to build our dataset, we utilize two types of assets: scene and object. We use the recently released Habitat-Matterport 3D dataset [29] as our scene assets. Those scenes are high quality capturing of real-world indoor scenes. We use Amazon-Berkeley Object [10] dataset as our object assets, because it comes with high-quality texture and accurate geometry. Since their provided meshes are not all watertight and may contain some internal structures, we follow the procedure of OccNet [26] to render hundreds of depth maps covering the object surface, then running TSDF-Fusion and marching cube [22] to get the water-tight mesh.

Pipeline. The overall procedure of creating synthetic scans goes as follows. We randomly choose a scene and an object. Then we find a placement location of such an object in that scene by sampling the navigable position [25, 36] in the scene. We avoid physical collision between the inserted object and the rest of the scene by ensuring there is an empty region in the surrounding of the chosen location. We also make sure that the object is placed on the floor of the scene instead of hovering in the air by running a few steps of physical simulation. We then sample a set of camera pose around the inserted object and ensure that

Method	Real	Multi-view	Realistic Object	Realistic Scene	Cam Pose	3D Model
Pix3D [35]	✓	✗	✓	✓	✓	✓
Redwood [8]	✓	✓	✓	✓	✗	✗
Objectron [1]	✓	✓	✓	✓	✓	✗
ShapeNet Choy [9]	✗	✓	✗	✗	✓	✓
ShapeNet DISN [9]	✗	✓	✗	✗	✓	✓
Things3D [42]	✗	✓	✗	✗	✓	✓
HM3D-ABO (Ours)	✗	✓	✓	✓	✓	✓

Table 1. Comparison of the existing object-centric datasets with our proposed HM3D-ABO dataset. We compare based on whether it contains real or synthetic capture (Real), multi-view capture (Multi-view), realistic object (Realistic Object), realistic background scene (Realistic Scene), camera pose annotation (Cam Pose), and accurate 3D model for the object (3D Model).

the camera does not collide with the scene. We then render the image at each location using habitat-sim [25, 36]’s built-in renderer. After rendering, we do a post-filtering to filter out low-quality capture. We calculate the ratio of the area of the bounding rectangle of the object mask to the size of the image and filter out images that have a ratio less than 0.2. Finally, we use the physical-based rendering engine Blender Cycles [11] to render the filtered configurations at 640×480 resolution. Each image takes around 10 seconds to render using one NVIDIA V100 GPU.

Statistics. HM3D-ABO has 1966 objects placed in 500 indoor scenes. In total, there are 3196 scene-shape configurations. In Fig. 1 we show qualitative comparisons between HM3D-ABO and existing object-centric multi-view datasets. More examples of our dataset are shown in Fig. 3.

3. Benchmark

We benchmark two tasks with the HM3D-ABO dataset: absolute camera pose estimation and few-view 3D object reconstruction. Our experimental setup follows FvOR [47].

3.1. Camera Pose Estimation

Camera pose estimation is a core step of many multi-view 3D reconstruction algorithm. Camera pose estimation approaches can be categorized into two types, i.e. relative pose approach and absolute pose approach. Relative pose approach estimates the relative pose between an image pair. Traditional approach relies on matching hand-crafted key-points [4, 17, 23], which could not handle much appearance variation and requires large overlap between image pair. The advance of deep learning also leads to algorithms that reduce the sensitivity to appearance change and low visual overlap [6, 18, 24, 31–34, 46, 48]. The second type is more tight to object-centric scenario. The absolute camera pose approach directly estimates the camera pose w.r.t. the canonical object coordinate system [43, 47]. Compared to relative pose estimation, these type of methods may be less generalizable compared to relative pose approach due to the assumption of canonical object coordinate system. But they are usually simpler as they directly output the camera poses for each image, without the need to perform pairwise rel-

Method	Pixel Error↓	Rot Error(°)↓	Trans Error(cm)↓
DISN [43]	23.0/9.6	18.6/4.1	9.1/6.2
Cai <i>et al.</i> [6]	38.9/18.0	31.3/7.7	12.3/9.9
FvOR-Pose [47]	18.0/5.0	14.3/1.3	7.6/5.0

Table 2. Absolute camera pose estimation results on HM3D-ABO dataset. We show the mean/median statistics for all metrics.

ative camera pose estimation followed by synchronization step to get absolute camera pose.

Here we provide a benchmark of absolute camera pose estimation. The input is a bag of RGB images capturing an object, and the output is the absolute camera pose for each of the images, w.r.t the canonical object coordinate. We follow the experimental setup of FvOR [43, 47] and use 4 images as input. We report the mean and median pixel error, rotation error, and translation error for each algorithm. The pixel error is computed w.r.t a 512×384 input image. We benchmark three methods as in [47]. The first one is based on DISN [43] which parametrizes camera poses by orthogonal vectors. The second one is based on Cai *et al.* [6] which use a classification plus regression approach. The last one we run is from FvOR [47]’s pose initialization module(denoted as FvOR-Pose in the following text), which uses a scene-coordinate as intermediate pose representation followed by RANSAC PnP [5] for pose extraction. The results can be found in Table 2.

3.2. Few-view 3D Object Reconstruction

Traditional research on 3D object reconstruction mainly focuses on SfM (structure-from-motion) pipelines from dense views, which are difficult to acquire for many applications. Single-view 3D reconstruction [13, 15, 16, 20, 26, 38, 40] receive a lot attention in recent years, but their reconstruction quality is often found to be limited [37]. Few-view 3D Object Reconstruction recovers the shape of the underlying object given a few RGB observations. Such a setting strikes a balance between capture complexity and reconstruction accuracy, and has been studied in several prior works [3, 9, 42, 43, 47, 51].

Existing approaches can be categorized into three types. The first type does not use camera pose for each image, such as 3D-R2N2 [9] and OccNet[†], which is an multi-

Method	GT		Noise@L1		Noise@L2		Noise@L3		Predict	
	IoU \uparrow	Chamfer-L1 \downarrow	IoU \uparrow	Chamfer-L1 \downarrow	IoU \uparrow	Chamfer-L1 \downarrow	IoU \uparrow	Chamfer-L1 \downarrow	IoU \uparrow	Chamfer-L1 \downarrow
OccNet † [3, 26]	0.762/0.812	2.01/1.63	0.762/0.812	2.01/1.63	0.762/0.812	2.01/1.63	0.762/0.812	2.01/1.63	0.762/0.812	2.01/1.63
IDR [49]	0.645/0.677	3.67/2.78	0.643/0.684	3.75/2.90	0.642/0.679	3.70/2.84	0.638/0.665	3.78/3.00	0.612/0.650	4.40/3.37
FvOR w/ GT Pose [47]	0.861/0.891	0.791/0.680	0.821/0.863	1.22/1.05	0.761/0.815	2.04/1.76	0.703/0.768	2.90/2.47	0.816/0.870	1.40/0.93
FvOR w/o Joint [47]	0.859/0.889	0.855/0.741	0.849/0.882	0.944/0.825	0.819/0.864	1.28/1.16	0.776/0.831	1.90/1.65	0.834/0.877	1.21/0.886
FvOR [47]	0.853/0.885	0.921/0.793	0.852/0.883	0.941/0.806	0.849/0.880	0.980/0.843	0.845/0.876	1.05/0.897	0.839/0.878	1.19/0.867

Table 3. Evaluating the robustness of few-view 3D reconstruction on HM3D-ABO dataset (mean/median, top-2 results highlighted). We report the results using ground truth poses, perturbed poses with different perturbation levels, and predicted poses by FvOR-Pose. Chamfer-L1 is multiplied by 100.

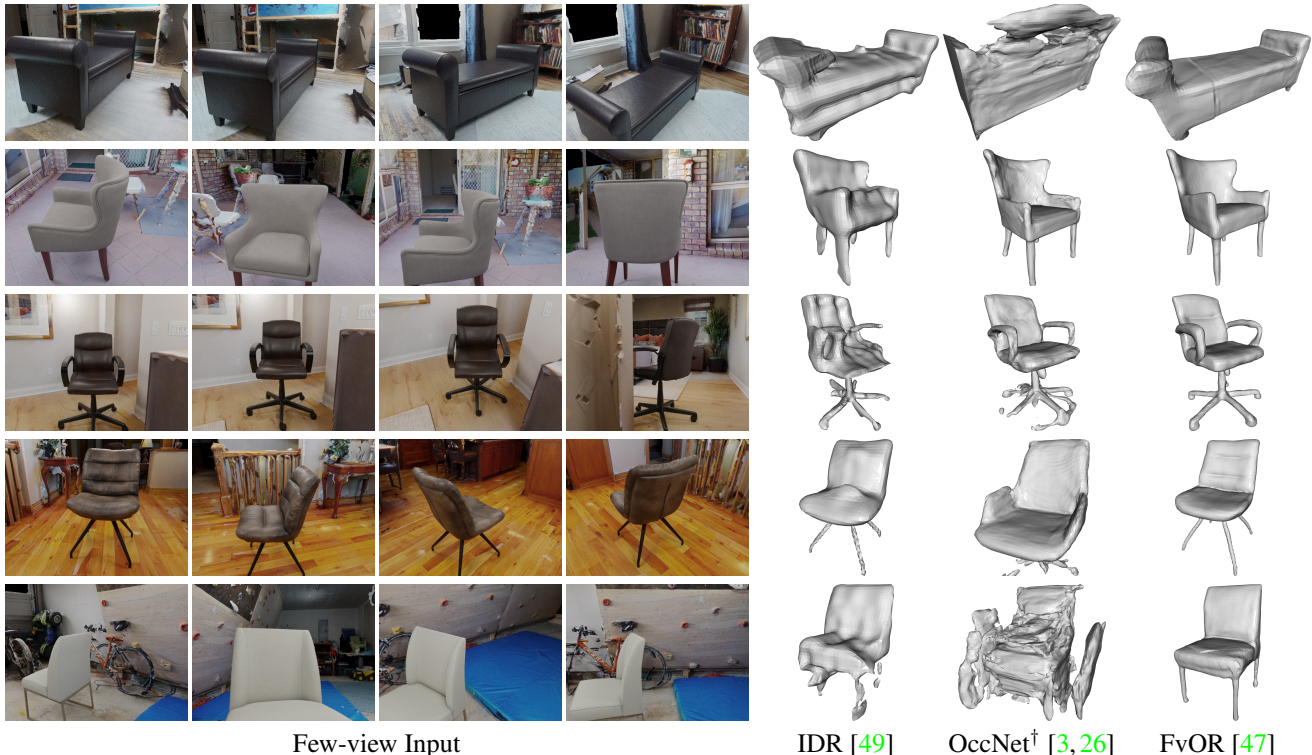


Figure 2. Qualitative comparisons between three approaches on HM3D-ABO. For each column, we show the 4 input views on the left and the reconstruction of each method on the right. FvOR [47] and IDR [49] use pose predicted by FvOR-Pose [47].

view version implementation of OccNet [26] proposed by 3D43D [3]. The second type assume known camera pose, such as 3D43D [3] and FvOR w/ GT Pose [47]. The other type uses the estimated camera pose, such as FvOR [47]. In particular, we experimented with the following baselines:

OccNet † [3, 26]. This is a multi-view version of OccNet [26] by 3D43D [3]. It does not require camera pose.

IDR [49] is an optimization-based algorithm that does not learn a prior from training data. IDR achieves good performance when reconstructing objects with tens of images paired with ground truth object masks. We run IDR [49] on each test input for 1000 epochs for best results.

FvOR w/ GT Pose is FvOR [47]’s standalone 3D reconstruction module trained with ground truth camera poses.

FvOR w/o Joint is FvOR [47]’s approach without performing joint refinement.

FvOR is FvOR [47]’s approach with joint refinement.

During training, for each scene-object pair, we randomly

select 4 views to form an input set. For testing, we select one bag of 4 views from each scene-object pair, yielding 500 testing examples in total. We compare the IoU metric and the Chamfer-L1 metric [26, 47]. To evaluate the shape quality invariant to similarity transform, we follow the procedure of FvOR [47] to find the similarity transform that aligns the predicted shape and G.T. shape before evaluation. We also follow FvOR [47] and compare all methods under three pose initialization settings. The first setting assumes we have access to the G.T. camera pose. The second setting assumes we have G.T. pose corrupted by different magnitudes of Gaussian noise. The pose perturbation magnitude is controlled by $\sigma \in \{0.75e-2, 1.5e-2, 2.25e-2\}$ with three values (called Noise@L1, Noise@L2, and Noise@L3 respectively). The last setting uses predicted camera pose by FvOR [47]’s pose initialization module FvOR-Pose. Note that these three pose initialization settings do not affect OccNet † as it does not utilize the camera pose at all.

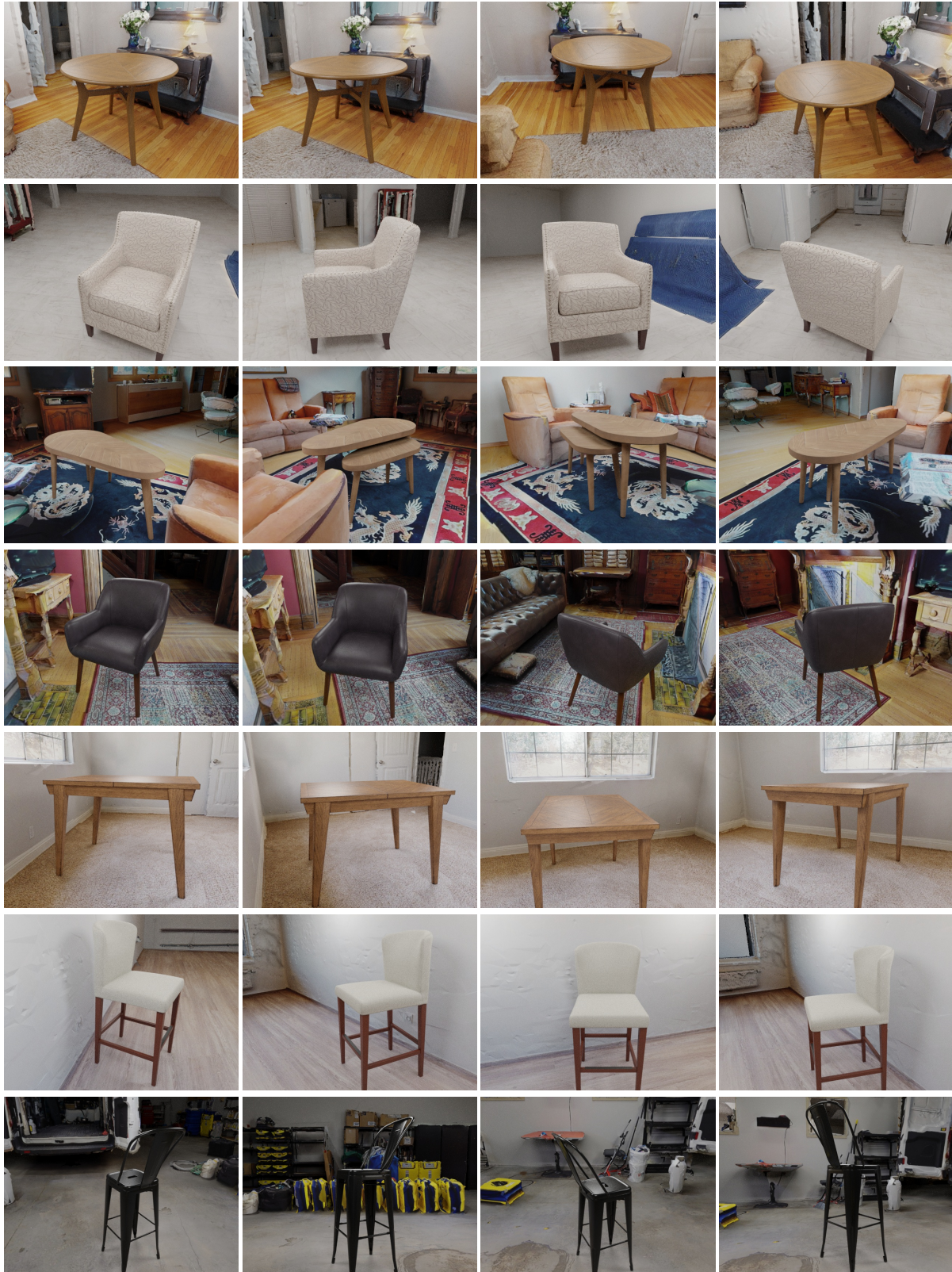


Figure 3. Examples of HM3D-ABO dataset. 3D assets from Amazon-Berkeley Object dataset [10] are placed in scenes from Habitat-Matterport 3D dataset [29] in a physically plausible way. For each object-scene configuration we render multiple images around the object. We show here for each configuration only 4 out of tens views.

The quantitative results can be found in Table 3. FvOR performs the best under most of the settings. IDR does not give satisfying results, which is probably due to the too-few input views. Pose-free method OccNet[†] gives decent results, and the fact that they do not need to estimate camera pose at all makes their method much simpler.

4. Discussion

In this report, we introduced a pipeline to create a photo-realistic object-centric dataset, HM3D-ABO. The synthesized images have realistic object and backgrounds compared to dataset based on ShapeNet [9, 43] and synthetic scene [42]. It also comes with high quality 3D models which are absent from several real-captured object-centric datasets [1, 8, 30, 35]. Such a dataset can be used for multiple purposes, for example, evaluating algorithms for few-view 3D reconstruction, novel-view synthesis, and camera pose estimation.

While we argue the HM3D-ABO dataset is a more realistic dataset than the previous synthetic object-centric datasets, we also note several limitations. First, the object assets are limited in terms of category. In the current version, most of the objects are chairs and tables, which are the major categories in ABO [10] dataset. With the increased object-level assets we could also expand our HM3D-ABO dataset. Secondly, the current object placement scheme is limited. We only place the single object on an empty region of the walkable surface, which does not include some more challenging scenarios that could also happen in practice, such as reconstructing a teddy bear sitting on the sofa.

References

- [1] Adel Ahmadyan, Liangkai Zhang, Artsiom Ablavatski, Jianing Wei, and Matthias Grundmann. Objectron: A large scale dataset of object-centric videos in the wild with pose annotations. In *Proceedings of the IEEE/CVF Conference on Computer Vision and Pattern Recognition*, pages 7822–7831, 2021. 1, 2, 5
- [2] Armen Avetisyan, Manuel Dahnert, Angela Dai, Manolis Savva, Angel X. Chang, and Matthias Niessner. Scan2cad: Learning cad model alignment in rgb-d scans. In *The IEEE Conference on Computer Vision and Pattern Recognition (CVPR)*, June 2019. 1
- [3] Miguel Ángel Bautista, Walter Talbott, Shuangfei Zhai, Nitish Srivastava, and Joshua M. Susskind. On the generalization of learning-based 3D reconstruction. *IEEE Winter Conference on Applications of Computer Vision (WACV)*, 2021. 1, 2, 3
- [4] Herbert Bay, Tinne Tuytelaars, and Luc Van Gool. Surf: Scaled up robust features. In *European conference on computer vision*, pages 404–417. Springer, 2006. 2
- [5] G. Bradski. The OpenCV Library. *Dr. Dobb’s Journal of Software Tools*, 2000. 2
- [6] Ruojin Cai, Bharath Hariharan, Noah Snavely, and Hadar Averbuch-Elor. Extreme rotation estimation using dense correlation volumes. In *Proceedings of the IEEE Conference on Computer Vision and Pattern Recognition (CVPR)*, pages 14566–14575, 2021. 2
- [7] Angel X. Chang, Thomas A. Funkhouser, Leonidas J. Guibas, Pat Hanrahan, Qi-Xing Huang, Zimo Li, Silvio Savarese, Manolis Savva, Shuran Song, Hao Su, Jianxiong Xiao, Li Yi, and Fisher Yu. Shapenet: An information-rich 3d model repository. *CoRR*, abs/1512.03012, 2015. 1
- [8] Sungjoon Choi, Qian-Yi Zhou, Stephen Miller, and Vladlen Koltun. A large dataset of object scans. *arXiv:1602.02481*, 2016. 1, 2, 5
- [9] Christopher B Choy, Danfei Xu, JunYoung Gwak, Kevin Chen, and Silvio Savarese. 3D-R2N2: A unified approach for single and multi-view 3d object reconstruction. In *Proceedings of the European Conference on Computer Vision (ECCV)*, 2016. 1, 2, 5
- [10] Jasmine Collins, Shubham Goel, Achleshwar Luthra, Leon Xu, Kenan Deng, Xi Zhang, Tomas F Yago Vicente, Himanshu Arora, Thomas Dideriksen, Matthieu Guillaumin, and Jitendra Malik. Abo: Dataset and benchmarks for real-world 3d object understanding. *arXiv preprint arXiv:2110.06199*, 2021. 1, 4, 5
- [11] Blender Online Community. *Blender - a 3D modelling and rendering package*. Blender Foundation, Stichting Blender Foundation, Amsterdam, 2018. 2
- [12] Laura Downs, Anthony Francis, Nate Koenig, Brandon Kinman, Ryan Hickman, Krista Reymann, Thomas B McHugh, and Vincent Vanhoucke. Google scanned objects: A high-quality dataset of 3d scanned household items. *arXiv preprint arXiv:2204.11918*, 2022. 1
- [13] Haoqiang Fan, Hao Su, and Leonidas J Guibas. A point set generation network for 3D object reconstruction from a single image. In *Proceedings of the IEEE Conference on Computer Vision and Pattern Recognition (CVPR)*, pages 605–613, 2017. 2
- [14] Ruohan Gao, Yen-Yu Chang, Shivani Mall, Li Fei-Fei, and Jiajun Wu. Objectfolder: A dataset of objects with implicit visual, auditory, and tactile representations. *arXiv preprint arXiv:2109.07991*, 2021. 1
- [15] Rohit Girdhar, David F Fouhey, Mikel Rodriguez, and Abhinav Gupta. Learning a predictable and generative vector representation for objects. In *Proceedings of the European Conference on Computer Vision (ECCV)*, pages 484–499. Springer, 2016. 2
- [16] Thibault Groueix, Matthew Fisher, Vladimir G Kim, Bryan C Russell, and Mathieu Aubry. A papier-mâché approach to learning 3D surface generation. In *Proceedings of the IEEE Conference on Computer Vision and Pattern Recognition (CVPR)*, pages 216–224, 2018. 2
- [17] Chris Harris, Mike Stephens, et al. A combined corner and edge detector. In *Alvey vision conference*, volume 15, pages 10–5244. Citeseer, 1988. 2
- [18] Linyi Jin, Shengyi Qian, Andrew Owens, and David F Fouhey. Planar surface reconstruction from sparse views. In *Proceedings of the IEEE/CVF International Conference on Computer Vision*, pages 12991–13000, 2021. 2
- [19] Abhishek Kar, Christian Häne, and Jitendra Malik. Learning a multi-view stereo machine. In *Advances in Neural Information Processing Systems (NeurIPS)*, pages 364–375, 2017. 1
- [20] Abhishek Kar, Shubham Tulsiani, Joao Carreira, and Jitendra Malik. Category-specific object reconstruction from a single image. In *Proceedings of the IEEE Conference on Computer Vision and Pattern Recognition (CVPR)*, pages 1966–1974, 2015. 2

- [21] Abhijit Kundu, Yin Li, and James M Rehg. 3d-rcnn: Instance-level 3d object reconstruction via render-and-compare. In *Proceedings of the IEEE Conference on Computer Vision and Pattern Recognition (CVPR)*, pages 3559–3568, 2018. 1
- [22] William E Lorensen and Harvey E Cline. Marching cubes: A high resolution 3d surface construction algorithm. *ACM siggraph computer graphics*, 21(4):163–169, 1987. 1
- [23] David G Lowe. Distinctive image features from scale-invariant keypoints. *International journal of computer vision*, 60(2):91–110, 2004. 2
- [24] Wei-Chiu Ma, Anqi Joyce Yang, Shenlong Wang, Raquel Urtasun, and Antonio Torralba. Virtual correspondence: Humans as a cue for extreme-view geometry. In *Proceedings of the IEEE/CVF Conference on Computer Vision and Pattern Recognition (CVPR)*, pages 15924–15934, June 2022. 2
- [25] Manolis Savva*, Abhishek Kadian*, Oleksandr Maksymets*, Yili Zhao, Erik Wijmans, Bhavana Jain, Julian Straub, Jia Liu, Vladlen Koltun, Jitendra Malik, Devi Parikh, and Dhruv Batra. Habitat: A Platform for Embodied AI Research. In *Proceedings of the IEEE/CVF International Conference on Computer Vision (ICCV)*, 2019. 1, 2
- [26] Lars Mescheder, Michael Oechsle, Michael Niemeyer, Sebastian Nowozin, and Andreas Geiger. Occupancy networks: Learning 3d reconstruction in function space. In *Proceedings of the IEEE Conference on Computer Vision and Pattern Recognition (CVPR)*, pages 4460–4470, 2019. 1, 2, 3
- [27] Michael Oechsle, Songyou Peng, and Andreas Geiger. Unisurf: Unifying neural implicit surfaces and radiance fields for multi-view reconstruction. *Proceedings of the IEEE International Conference on Computer Vision (ICCV)*, 2021. 1
- [28] Sida Peng, Yuanqing Zhang, Yinghao Xu, Qianqian Wang, Qing Shuai, Hujun Bao, and Xiaowei Zhou. Neural body: Implicit neural representations with structured latent codes for novel view synthesis of dynamic humans. *Proceedings of the IEEE Conference on Computer Vision and Pattern Recognition (CVPR)*, 2021. 1
- [29] Santhosh K Ramakrishnan, Aaron Gokaslan, Erik Wijmans, Oleksandr Maksymets, Alex Clegg, John Turner, Eric Undersander, Wojciech Galuba, Andrew Westbury, Angel X Chang, et al. Habitat-Matterport 3D dataset (HM3D): 1000 large-scale 3D environments for embodied ai. *arXiv preprint arXiv:2109.08238*, 2021. 1, 4
- [30] Jeremy Reizenstein, Roman Shapovalov, Philipp Henzler, Luca Sbordone, Patrick Labatut, and David Novotny. Common objects in 3D: Large-scale learning and evaluation of real-life 3d category reconstruction. In *Proceedings of the IEEE/CVF International Conference on Computer Vision (ICCV)*, pages 10901–10911, October 2021. 1, 5
- [31] Paul-Edouard Sarlin, Daniel DeTone, Tomasz Malisiewicz, and Andrew Rabinovich. SuperGlue: Learning feature matching with graph neural networks. In *Proceedings of the IEEE/CVF conference on computer vision and pattern recognition*, pages 4938–4947, 2020. 2
- [32] Mohammad Amin Shabani, Weilian Song, Makoto Odamaki, Hirochika Fujiki, and Yasutaka Furukawa. Extreme structure from motion for indoor panoramas without visual overlaps. In *Proceedings of the IEEE/CVF International Conference on Computer Vision*, pages 5703–5711, 2021. 2
- [33] Che Sun, Yunde Jia, Yi Guo, and Yuwei Wu. Global-aware registration of less-overlap rgb-d scans. In *Proceedings of the IEEE/CVF Conference on Computer Vision and Pattern Recognition*, pages 6357–6366, 2022. 2
- [34] Jiaming Sun, Zehong Shen, Yuang Wang, Hujun Bao, and Xiaowei Zhou. Loftr: Detector-free local feature matching with transformers. In *Proceedings of the IEEE Conference on Computer Vision and Pattern Recognition (CVPR)*, pages 8922–8931, 2021. 2
- [35] Xingyuan Sun, Jiajun Wu, Xiuming Zhang, Zhoutong Zhang, Chengkai Zhang, Tianfan Xue, Joshua B Tenenbaum, and William T Freeman. Pix3d: Dataset and methods for single-image 3d shape modeling. In *IEEE Conference on Computer Vision and Pattern Recognition (CVPR)*, 2018. 1, 2, 5
- [36] Andrew Szot, Alex Clegg, Eric Undersander, Erik Wijmans, Yili Zhao, John Turner, Noah Maestre, Mustafa Mukadam, Devendra Chaplot, Oleksandr Maksymets, Aaron Gokaslan, Vladimir Vondrus, Sameer Dharur, Franziska Meier, Wojciech Galuba, Angel Chang, Zsolt Kira, Vladlen Koltun, Jitendra Malik, Manolis Savva, and Dhruv Batra. Habitat 2.0: Training home assistants to rearrange their habitat. In *Advances in Neural Information Processing Systems (NeurIPS)*, 2021. 1, 2
- [37] Maxim Tatarchenko, Stephan R Richter, René Ranftl, Zhuwen Li, Vladlen Koltun, and Thomas Brox. What do single-view 3D reconstruction networks learn? In *Proceedings of the IEEE Conference on Computer Vision and Pattern Recognition (CVPR)*, pages 3405–3414, 2019. 2
- [38] Nanyang Wang, Yinda Zhang, Zhuwen Li, Yanwei Fu, Wei Liu, and Yu-Gang Jiang. Pixel2mesh: Generating 3D mesh models from single RGB images. In *Proceedings of the European Conference on Computer Vision (ECCV)*, pages 52–67, 2018. 2
- [39] Peng Wang, Lingjie Liu, Yuan Liu, Christian Theobalt, Taku Komura, and Wenping Wang. Neus: Learning neural implicit surfaces by volume rendering for multi-view reconstruction. *Advances in Neural Information Processing Systems (NeurIPS)*, 2021. 1
- [40] Jiajun Wu, Tianfan Xue, Joseph J Lim, Yuandong Tian, Joshua B Tenenbaum, Antonio Torralba, and William T Freeman. Single image 3D interpreter network. In *Proceedings of the European Conference on Computer Vision (ECCV)*, pages 365–382. Springer, 2016. 2
- [41] Zhirong Wu, Shuran Song, Aditya Khosla, Fisher Yu, Linguang Zhang, Xiaoou Tang, and Jianxiong Xiao. 3d shapenets: A deep representation for volumetric shapes. In *Proceedings of the IEEE conference on computer vision and pattern recognition*, pages 1912–1920, 2015. 1
- [42] Haozhe Xie, Hongxun Yao, Shengping Zhang, Shangchen Zhou, and Wenxiu Sun. Pix2vox++: multi-scale context-aware 3d object reconstruction from single and multiple images. *International Journal of Computer Vision (IJCV)*, 128(12):2919–2935, 2020. 1, 2, 5
- [43] Qiangeng Xu, Weiye Wang, Duygu Ceylan, Radomir Mech, and Ulrich Neumann. DISN: Deep implicit surface network for high-quality single-view 3d reconstruction. *Advances in Neural Information Processing Systems (NeurIPS)*, pages 492–502, 2019. 1, 2, 5
- [44] Mingyue Yang, Yuxin Wen, Weikai Chen, Yongwei Chen, and Kui Jia. Deep optimized priors for 3d shape modeling and reconstruction. In *Proceedings of the IEEE Conference on Computer Vision and Pattern Recognition (CVPR)*, pages 3269–3278, 2021. 1

- [45] Shichao Yang and Sebastian Scherer. Cubeslam: Monocular 3D object slam. *IEEE Transactions on Robotics*, 35(4):925–938, 2019. [1](#)
- [46] Zhenpei Yang, Jeffrey Z Pan, Linjie Luo, Xiaowei Zhou, Kristen Grauman, and Qixing Huang. Extreme relative pose estimation for rgb-d scans via scene completion. In *Proceedings of the IEEE Conference on Computer Vision and Pattern Recognition (CVPR)*, pages 4531–4540, 2019. [2](#)
- [47] Zhenpei Yang, Zhile Ren, Miguel Angel Bautista, Zaiwei Zhang, Qi Shan, and Qixing Huang. Fvor: Robust joint shape and pose optimization for few-view object reconstruction, 2022. [2](#), [3](#)
- [48] Zhenpei Yang, Siming Yan, and Qixing Huang. Extreme relative pose network under hybrid representations. In *Proceedings of the IEEE Conference on Computer Vision and Pattern Recognition (CVPR)*, pages 2455–2464, 2020. [2](#)
- [49] Lior Yariv, Yoni Kasten, Dror Moran, Meirav Galun, Matan Atzmon, Basri Ronen, and Yaron Lipman. Multiview neural surface reconstruction by disentangling geometry and appearance. *Advances in Neural Information Processing Systems (NeurIPS)*, 33, 2020. [3](#)
- [50] Alex Yu, Vickie Ye, Matthew Tancik, and Angjoo Kanazawa. pixelnerf: Neural radiance fields from one or few images. In *Proceedings of the IEEE Conference on Computer Vision and Pattern Recognition (CVPR)*, pages 4578–4587, 2021. [1](#)
- [51] Jason Y Zhang, Gengshan Yang, Shubham Tulsiani, and Deva Ramanan. Ners: Neural reflectance surfaces for sparse-view 3d reconstruction in the wild. *Advances in Neural Information Processing Systems (NeurIPS)*, 2021. [2](#)